iScience

Article

Mitochondrial ROS inhibition prevents doxorubicin-induced breast cancer cell migration and invasion

Graphical abstract

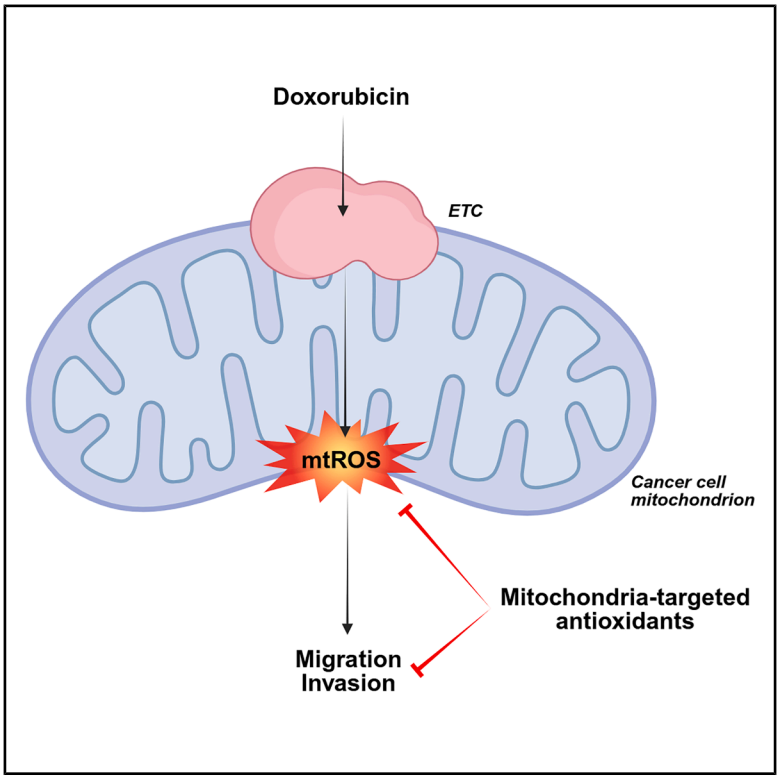

Authors

Tania Capeloa, Justine A. Van de Velde, Erica Pranzini, ..., Valéry L. Payen, Paolo E. Porporato, Pierre Sonveaux

Correspondence

paolo.porporato@unito.it (P.E.P.), pierre.sonveaux@uclouvain.be (P.S.)

In brief

Therapeutic procedure; Molecular network; Cancer systems biology

Highlights

- Doxorubicin induces mitochondrial ROS (mtROS) production in breast cancer cells
- Sublethal doses of doxorubicin promote breast cancer cell migration and invasion
- mtROS-targeting antioxidants prevent doxorubicin-induced migration and invasion
- MitoTEMPO prevents breast cancer metastasis in doxorubicin-treated mice

Capeloa et al., 2025, iScience *28*, 113031
August 15, 2025
https://doi.org/10.1016/j.isci.2025.113031

CellPress

iScience

CellPress
OPEN ACCESS

Article

Mitochondrial ROS inhibition prevents doxorubicin-induced breast cancer cell migration and invasion

Tania Capeloa,[1,8] Justine A. Van de Velde,[1,8] Erica Pranzini,[1,2] Luigi Ippolito,[1,2] Luca X. Zampieri,[1] Morgane Tardy,[1,3] Thibaut Vazeille,[1] Alan Provito,[1] Giovanna Carrà,[4,7] Alfonso Scalera,[5] Valéry L. Payen,[1] Paolo E. Porporato,[1,5,*] and Pierre Sonveaux[1,6,9,*]

[1]Pole of Pharmacology and Therapeutics, Institut de Recherche Expérimentale et Clinique (IREC), Université catholique de Louvain (UCLouvain), 1200 Brussels, Belgium
[2]Department of Experimental and Clinical Biomedical Sciences Mario Serio, University of Florence, 50134 Firenze, Italy
[3]Inserm U1019, CNRS UMR9017, Institut Pasteur de Lille, 59000 Lille, France
[4]Department of Clinical and Biological Sciences, Molecular Biotechnology Center (MBC), University of Turin, 10126 Turin, Italy
[5]Department of Molecular Biotechnology and Health Science, Molecular Biotechnology Center (MBC), University of Turin, 10126 Turin, Italy
[6]WEL Research Institute, WELBIO Department, 1300 Wavre, Belgium
[7]San Luigi Gonzaga Hospital, 10043 Orbassano, Italy
[8]These authors contributed equally
[9]Lead contact
*Correspondence: paolo.porporato@unito.it (P.E.P.), pierre.sonveaux@uclouvain.be (P.S.)
https://doi.org/10.1016/j.isci.2025.113031

SUMMARY

For cancer patients, metastasis is a life-threatening event limiting therapeutic options. Molecularly, the metastatic phenotype can be conferred by mitochondrial reactive oxygen species (mtROS) generated upon metabolic stress. Mitochondrial damage can also trigger mtROS production, which is particularly well illustrated for anthracyclines. Here, we tested in mouse models of murine and human breast cancer whether this type of chemotherapy can trigger metastasis. We report that subcytotoxic doses of doxorubicin mimicking the clinical situation in poorly perfused tumor areas sequential trigger mtROS production, activate TGFβ pathway effector Pyk2, and increase cancer cell migration and invasion. Fortunately, the metastatic switch was incompletely induced, and doxorubicin did not promote breast cancer metastasis in immunocompetent mice. Yet, MitoTEMPO fully prevented metastatic dissemination and did not interfere with doxorubicin cytotoxicity, making it attractive to combine anthracyclines with mitochondria-targeted antioxidants.

INTRODUCTION

In solid tumors, the occurrence of cancer metastasis marks the transition from a localized to a systemic disease. For patients, it is often associated with a change in therapeutic intentions from curative to palliative care, especially when tumors become polymetastatic. At that stage, localized interventions, including surgery and radiotherapy, are increasingly difficult to perform, and metastases are generally more resistant to anticancer therapies than the corresponding primary tumor.[1] Consequently, more than 65% of cancer-associated deaths are caused by progression to a metastatic disease, all cancer types combined.[2]

Breast cancer, especially hormone-independent HER2-positive and triple negative subtypes, are particularly prone to metastasis, which often develops during treatment.[3] While targeted therapies and immunotherapy offer some hope for cure through achieving metastatic regression and, sometimes, sterilization, there is currently no specific clinical treatment to prevent metastatic dissemination. This picture is particularly worrying, since more than 90% of breast cancer patients present no metastases at diagnosis.[3]

In advanced cancers, metastatic progenitor cells are a subpopulation of cancer cells possessing all the phenotypic features that are necessary to establish viable metastases. They are only a tiny minority among circulating tumor cells (CTCs), representing a fraction of ~1% of the entire CTC population.[4] They originate from metabolically hostile areas in primary tumors that are characterized by a limited nutrient (including oxygen) offer and metabolic waste accumulation acidifying the local microenvironment.[5] Metastatic progenitor cells thus represent the CTC subpopulation to target for metastatic prevention.

Using Darwinian selection to enrich their metastatic potential followed by a thorough metabolic characterization, we previously demonstrated that mitochondria within metastatic progenitor cells promote metastatic dissemination, acting as metabolic sensors and intracellular transducers of prometastatic signals.[6] Upon metabolic stress, mitochondria increase their production of mitochondrial reactive oxygen species (mtROS) to a subcytotoxic level, converting less aggressive cancer cells in metastatic

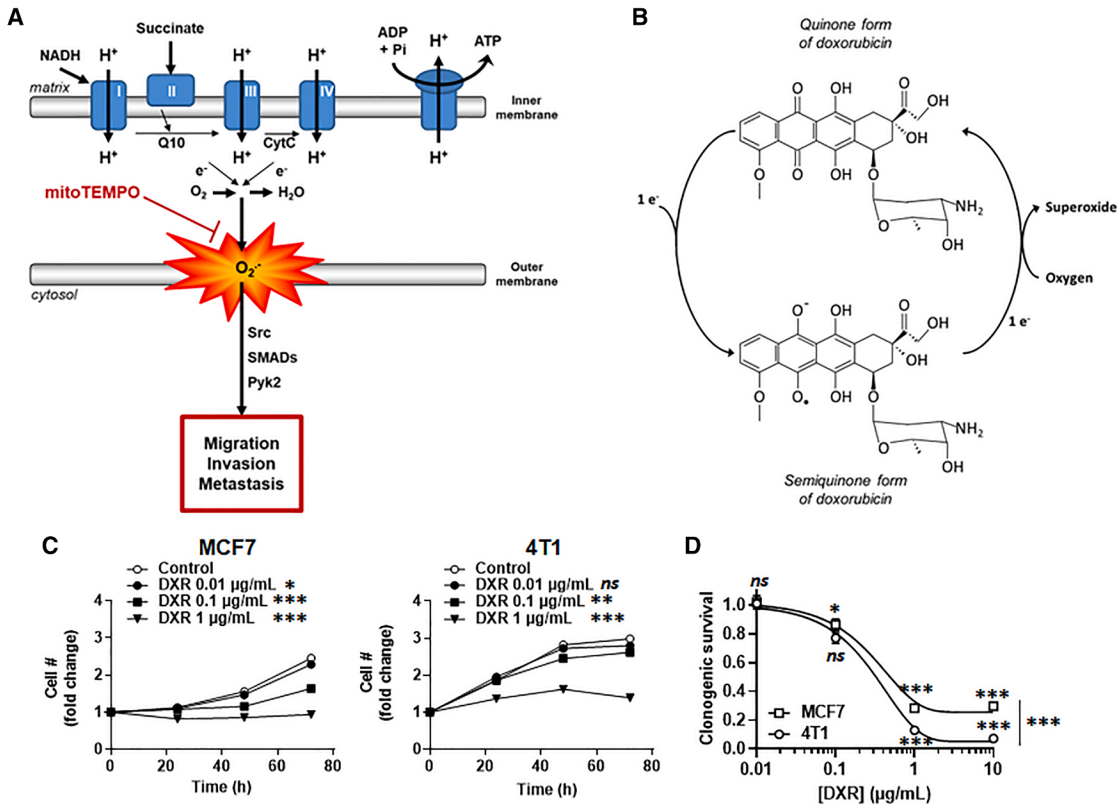

Figure 1. Human MCF7 breast cancer cells are more sensitive to doxorubicin than murine 4T1 breast cancer cells

(A) The scheme shows mitochondrial redox signaling in the promotion of cancer cell migration, invasion, and metastasis, based on refs. [6–8] Briefly, electron leak at the electron transport chain of metastatic progenitor cells results in the production of superoxide, triggering the downstream part of the prometastatic transforming growth factor β (TGFβ) pathway.

(B) Doxorubicin redox cycling generates superoxide. A single electron is captured by the quinone form of doxorubicin that is reduced to its semiquinone form, and then the electron is donated to oxygen, which regenerates the quinone form of doxorubicin and produces superoxide. Adapted from ref. [9]

(C) The number of human MCF7 (left, $n = 5$) and murine 4T1 (right, $n = 5$) breast cancer cells was determined over time upon treatment with increasing doses of doxorubicin (DXR). Data are represented as mean ± SEM. *ns* $p > 0.05$, *$p < 0.05$, **$p < 0.01$, ***$p < 0.005$, compared to respective controls by two-way ANOVA.

(D) The clonogenic survival of MCF7 ($n = 3$–5) and 4T1 ($n = 5$) cells was determined 16 h after treatment with increasing doses of doxorubicin (DXR). Data are represented as mean ± SEM. *ns* $p > 0.05$, *$p < 0.05$, ***$p < 0.005$. by two-way ANOVA with Sidak's post-hoc test.

progenitors (Figure 1A). This phenomenon is perhaps best illustrated by the observation that transferring mtROS-producing mitochondria from the latter to the former is sufficient to transfer the metastatic phenotype.[10] Conversely, antioxidant drugs selectively targeted to mitochondria have been shown to repress metastatic dissemination in orthotopic mouse models of human breast[6–8] and pancreatic[11] cancers. These drugs, including MitoTEMPO[12] and MitoQ,[13] possess a positively charged triphenylphosphonium (TPP^+) moiety ensuring their accumulation in negatively charged mitochondria, which is particularly the case in metastatic progenitor cells that are characterized by an enhanced electron leak from the mitochondrial electron transport chain (ETC).[7,8,11] Once at the inner mitochondrial membrane, leaking electrons react with the quinone antioxidant core of MitoTEMPO and MitoQ,[14] thus preventing mtROS production, hence metastasis in preclinical mouse models.[6–8,11] MitoQ singles out from other mitochondria-targeted antioxidants by the fact that it already successfully passed Phase I safety clinical trials,[15] making of this molecule a good candidate for metastasis prevention.

Not only mitochondrial signaling, but also mitochondrial damage, can lead to increased mtROS production.[16] This is particularly relevant for anthracycline-based chemotherapies used in breast cancer treatment, whose cardiotoxicity is essentially due to their capacity to induce mtROS production in cardiomyocytes (Figure 1B).[17,18] We therefore conceived that a same molecular response could occur in cancer cells exposed to subcytotoxic levels of anthracyclines, supporting the idea that inducing metastasis could be a side effect of suboptimal anthracycline dose delivery in poorly drained tumor areas. This pressing question was addressed using doxorubicin, known to be the most potent anthracycline to trigger mtROS production by cells (as it binds to cardiolipin in mitochondria),[19] and murine and human breast cancer cells, with MitoTEMPO and MitoQ as potential pharmacological solutions to prevent the metastatic phenotype. Doxorubicin concentration is further known to be highly variable spatially in human tumors, with areas exposed to therapeutic and others to subtherapeutic concentrations.[20] Here, we show that subcytotoxic doses of doxorubicin have this capacity

in mouse and human breast cancer cells, but not to the point of increasing the metastatic burden in immunocompetent mice bearing orthotopic breast cancers. Preclinical evidence is provided that mitochondria-targeted antioxidants can be safely used in combination with anthracyclines, as they do not interfere with their cytotoxicity and can fully prevent metastasis.

RESULTS

Identification of a suboptimal dose range of doxorubicin in breast cancer cells

To test whether a low dose of doxorubicin could promote breast cancer metastasis, we first aimed to determine a suboptimal concentration range of doxorubicin in human MCF7 and mouse 4T1 breast cancer cells. Direct cell count showed a partial decrease in cell numbers at doxorubicin concentrations from 0.01 to 0.1 μg/mL compared to 1 μg/mL where maximal effects were seen (Figure 1C). Similar results were obtained in clonogenic assays, with partial inhibition between 0.01 and 0.1 μg/mL, and full inhibition starting at 1 μg/mL doxorubicin (Figure 1D). Of note, MCF7 were more resistant than 4T1 cells to doxorubicin, with ∼25% of MCF7 cells still forming colonies at doxorubicin concentrations up to 10 μg/mL, while all 4T1 cells were sterilized at doxorubicin concentrations ≥1 μg/mL.

Sublethal concentrations of doxorubicin stimulate breast cancer cell respiration and the production of mitochondrial reactive oxygen species

In cardiomyocytes, doxorubicin accumulates in mitochondria where it binds to cardiolipin,[21] induces redox stress,[17,18] and alters several mitochondrial functions and activities, including cell respiration.[22] In MCF7 and 4T1 breast cancer cells treated for 24 h, we observed a bell-shape increase in oxygen consumption rates (OCRs), with sublethal doxorubicin concentrations of 0.01–0.1 μg/mL triggering basal and maximal mitochondrial OCR (mtOCR) in both cell lines, as well as proton leak (Figures 2A and 2B). This doxorubicin concentration range is clinically relevant.[23] Comparatively, exposure to a lethal concentration of doxorubicin (1 μg/mL) decreased mtOCR in 4T1 cells (Figure 2B), while surviving MCF7 cells kept the capacity to increase their maximal mtOCR (Figure 2A).

In general, increased basal OCR associated with moderate proton leak goes along with increased mitochondrial mtROS production.[24] Accordingly, measurements at the peak of OCRs showed a ∼2-fold increase in mtROS production (Figure 2C). Meanwhile, enzymatic measurements showed that MCF7 cells kept an unchanged glucose consumption rate with a decreased lactate consumption rate (Figure 2D), while 4T1 cells rather increased glucose uptake with unchanged lactate release.

Sublethal concentrations of doxorubicin trigger breast cancer cell migration

Because increased mtROS production can promote migration, invasion and metastasis,[6–8,11] we next tested the phenotypical consequences of low dose doxorubicin treatment on our breast cancer cell models. Upon exposure to 0.02 μg/mL doxorubicin for 2 weeks (Figure 3A) or 0.1 μg/mL doxorubicin for 24 h (Figure 3B), 4T1 cells showed remarkable changes in cell morphology, displaying a general enlargement of the cellular body and a higher number of protrusions. This phenomenon was previously described by Bandyopadhyay et al.[25] after longer incubation times, which they related to a partial epithelial to mesenchymal transition (EMT). Elongation was less obvious for MCF7 cells (Figure 3B), which nevertheless displayed a higher number of protrusions clearly seen on bright field images 2 weeks after exposure to 0.02 μg/mL doxorubicin (Figure 3A). Coherently with actin remodeling shown in Figure 3B, breast cancer cells exposed for 16 h to doxorubicin and left to recover for 6 h gained increased migratory activities (Figure 3C). 4T1 were more responsive than MCF7 to low-dose doxorubicin-induced cell migration, both at 0.01 and 0.1 μg/mL of the drug. In the same conditions, MCF7 cells treaded with 0.1 μg/mL doxorubicin showed increased mRNA expression of EMT markers *vimentin*, *zinc finger E-box-binding homeobox 1* (*ZEB1*), and *Slug*, but *E-cadherin* expression was also increased (Figure S1A), indicating partial EMT. Such hybrid epithelial/mesenchymal phenotype has previously been reported to be associated with enhanced plasticity and metastatic potential.[26] The EMT switch was more traditional in 4T1, with an increased expression of *N-cadherin*, but not of *E-cadherin* (Figure S1B).

Sublethal concentrations of doxorubicin activate the effector part of the TGFβ signaling pathway in breast cancer cells

In mouse melanoma as well as human cervix, breast, and pancreatic cancer cells,[6–8,11] we previously documented that mtROS, in particular mitochondrial superoxide ($mtO_2^{\cdot-}$), activate the effector part of the TGFβ signaling pathway. Molecularly, mtROS activate src kinase within mitochondria in a process where H_2O_2 acts as an intermediate[6] that oxidizes src on a specific cysteine residue (Cys277), thereby triggering src homodimerization, autophosphorylation on Tyr416, and activity.[27] Src then reaches the cytosol to sequentially activate SMAD4 and focal adhesion kinase Pyk2 (Y402 phosphorylation), which is the final effector that ultimately remodels the cell cytoskeleton to induce migration and invasion.[6,11,28,29] mtROS-induced activation of the TGFβ pathway thus bypasses the need of TGFβ to bind and activate its receptor. Similarly, doxorubicin at low dose (0.1 μg/mL, 24 h) activated Pyk2 in MCF7 cells, as detected using a specific anti-phospho-Y402-Pyk2 antibody in immunofluorescence imaging (Figure 4A). This response was inhibited by $mtO_2^{\cdot-}$ scavenger MitoTEMPO (Figure 4B), indicating that doxorubicin-induced Pyk2 activation is mtROS-dependent in these human breast cancer cells. Low dose doxorubicin (0.01 μg/mL) also activated Pyk2 (Y402 phosphorylation) in 4T1 cells, which was detected using western blotting (Figure 4C) and immunofluorescent staining (Figure 4D). It was inhibited by MitoTEMPO (Figures 4C and 4D), thus confirming that doxorubicin mtROS-dependently activates the final effector of the TGFβ signaling pathway in breast cancer cells.

Mitochondrial superoxide scavengers inhibit doxorubicin-induced breast cancer cell migration and invasion

Compared to general antioxidants that have unpredictable effects in cancer,[30] mitochondria-targeted superoxide scavengers

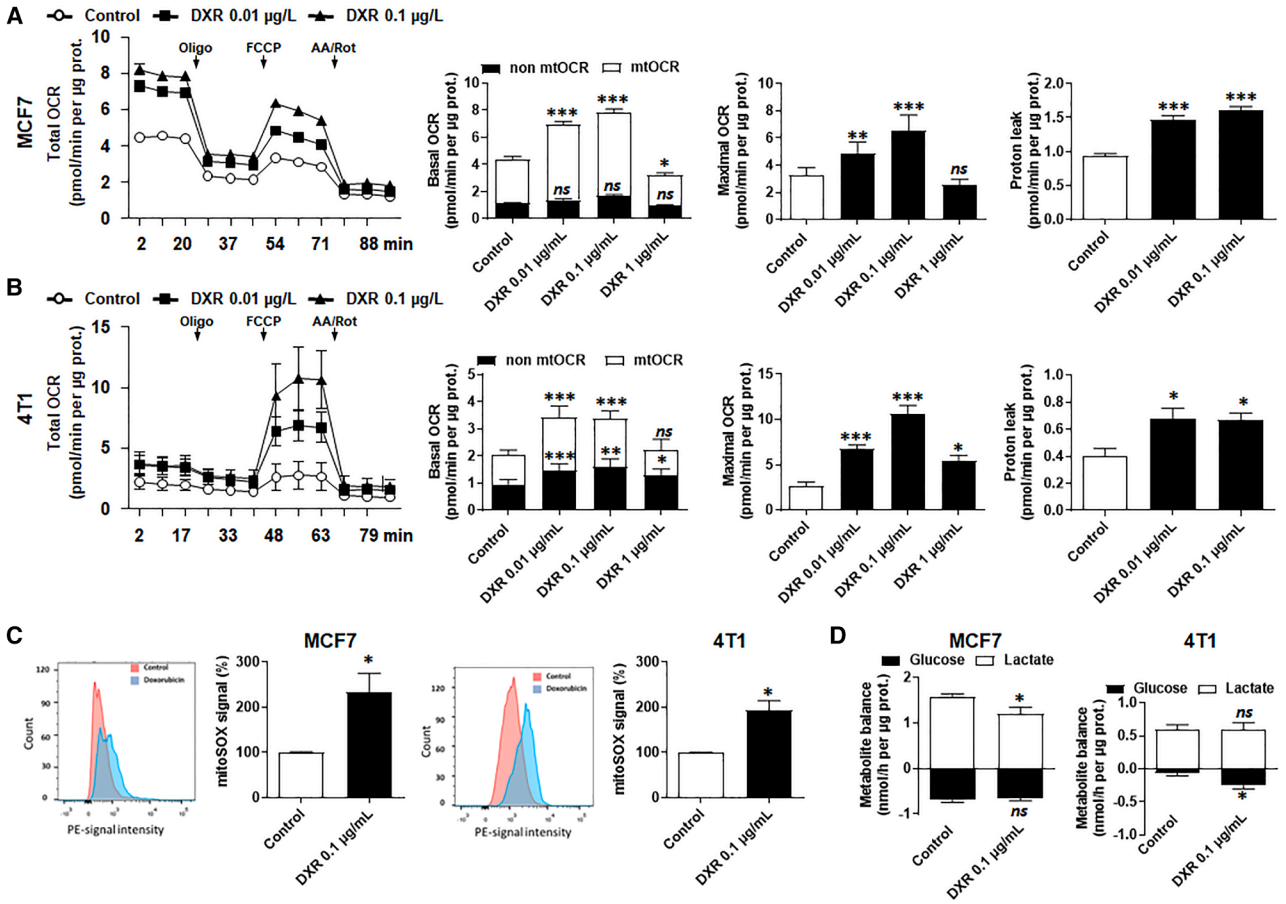

Figure 2. Subcytotoxic concentrations of doxorubicin stimulate breast cancer cell mitochondrial respiration and mtROS production

(A) Cells were treated with the indicated concentrations of doxorubicin (DXR) for 24 h. The oxygen consumption rate (OCR) of MCF7 breast cancer cells was measured with a Seahorse XF96 bioanalyzer (Agilent Technologies). Representative traces reporting on total OCR are shown on far left (Oligo, Oligomycin; FCCP, carbonyl cyanide-p-trifluoromethoxyphenylhydrazone; AA/Rot, Antimycin A + Rotenone), basal mitochondrial OCR (mtOCR) and non-mtOCR on middle left, maximal OCR on middle right, proton leak on far right (n = 7–8). All data were normalized by total protein content and are represented as mean ± SEM. *ns* $p > 0.05$, *$p < 0.05$, **$p < 0.01$, ***$p < 0.005$ compared to control, by one-way ANOVA followed by Dunnett's post hoc test.

(B) as in (A), but using murine 4T1 cancer cells. All data were normalized by total protein content and are represented as mean ± SEM. *ns* $p > 0.05$, *$p < 0.05$, **$p < 0.01$, ***$p < 0.005$ compared to control, by one-way ANOVA followed by Dunnett's post hoc test.

(C) Cells were treated with the indicated concentrations of DXR for 24 h. Mitochondrial ROS (mtROS) levels were measured in MCF7 (left, n = 5) and 4T1 (right, n = 3) cells by FACS analysis using mitochondria-targeted fluorescent probe mitoSOX. Representative graphs show data plotted population distributions. Graphs show the mean fluorescent intensity of the mitoSOX signal normalized to vehicle-treated cells (control). Data are represented as mean ± SEM. *$p < 0.05$, by Student's t test.

(D) Cells were treated with the indicated concentrations of DXR for 24 h. Glucose uptake and lactate release were measured enzymatically in MCF7 (left, n = 5–6) and 4T1 cells (right, n = 5–6). Data are represented as mean ± SEM. *ns* $p > 0.05$, *$p < 0.05$, by Student's t test.

MitoTEMPO and MitoQ selectively inhibit mitochondrial redox signaling,[12,15,31,32] including in cancer cells.[6–8,11] Importantly, at a concentration of 50 μM, MitoTEMPO did not interfere with doxorubicin-induced MCF7 and 4T1 cancer cell death measured 48 h after treatment using a viability assay reporting on intracellular ATP content (Figure 5A). This observation indicated that redox cycling does not participate in the anticancer activities of doxorubicin in our model cell lines. Comparatively, MitoTEMPO at the same 50 μM concentration blocked doxorubicin (0.1 μg/mL)-induced MCF7 and 4T1 cancer cell migration (Figure 5B) and invasion (Figure 5C). Compared to doxorubicin alone, the combination treatment was associated with decreased basal mtOCR (Figure S2). Of note, MitoTEMPO alone did not interfere with basal cell migration (Figure 5B) nor basal invasion (Figure 5C).

To validate our results, we used murine 168FARN breast cancer cells as a third model. MitoTEMPO (50 μM, 48 h) did not interfere with, but rather improved, doxorubicin-induced cell killing (Figure S3A). It repressed doxorubicin-induced 168FARN cancer cell migration (Figure S3B) and invasion (Figure S3C).

To further generalize our results to other mitochondria-targeted antioxidants, we used MitoQ, which acts as a chain breaker to stop mitochondrial redox signaling.[7,8,15] Similar to MitoTEMPO (see Figure 4C), MitoQ (100 nM) inhibited doxorubicin-induced

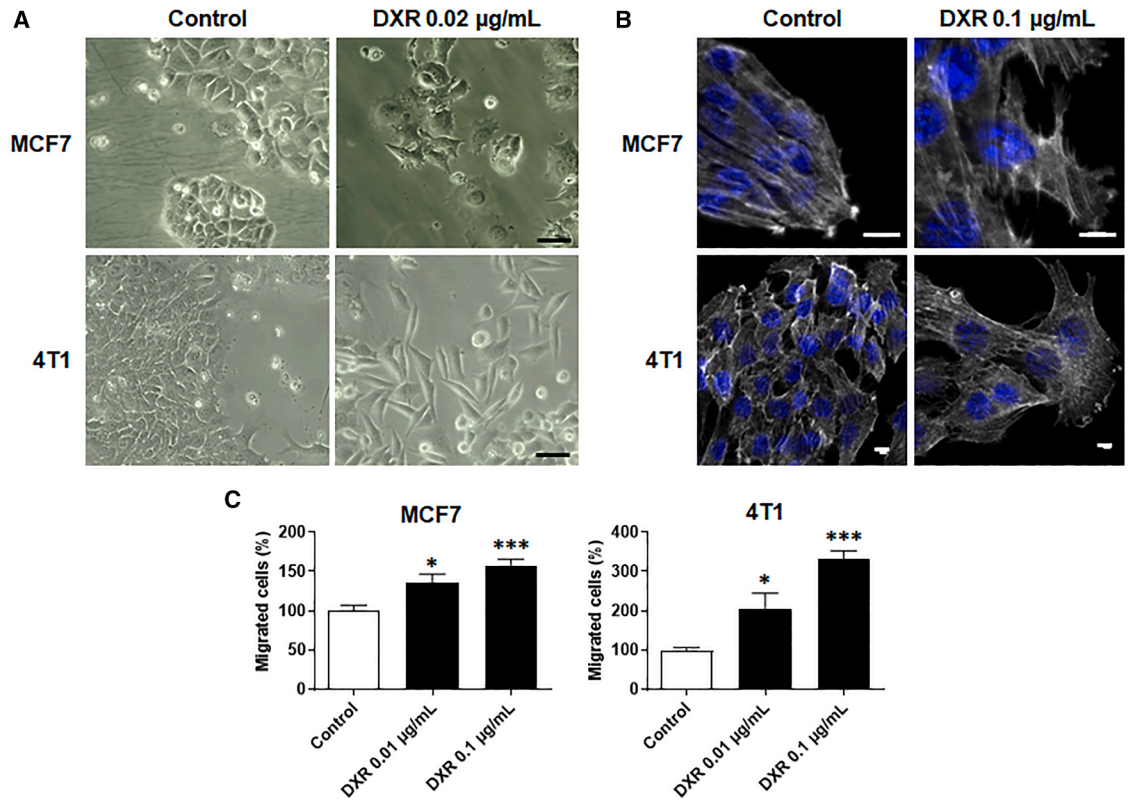

Figure 3. Subcytotoxic concentrations of doxorubicin promote breast cancer cell migration

(A) Representative bright field pictures of MCF7 and 4T1 breast cancer cells treated for 2 weeks with 0.02 µg/mL doxorubicin (DXR). Bars = 100 µm.

(B) Representative microscopy pictures of MCF7 and 4T1 cells treated for 24 h ± 0.1 µg/mL DXR. The cytoskeleton is stained with DyLight 488 phalloidin (white) and nuclei with DAPI (blue). Bars = 10 µM.

(C) Cells were pretreated with the indicated amounts DXR for 16 h, and left to recover for 6 h. The graphs show MCF7 (left, $n = 6$) and 4T1 (right, $n = 6$) cell migration toward serum used as a chemoattractant, quantified using a NeuroProbe chemotaxis chamber. Data are represented as mean ± SEM. *ns* $p > 0.05$, *$p < 0.05$, ***$p < 0.005$ compared to respective controls, by one-way ANOVA followed by Dunnett's post hoc test.

See also Figure S1.

PYK2 activation in 4T1 cells (Figure S3D). It did not interfere with doxorubicin-induced MCF7 and 4T1 cancer cell killing (100 nM, 48 h) (Figure S3E), but it repressed doxorubicin (0.1 µg/mL)-induced MCF7 and 4T1 cell migration (Figure S3F) and invasion (Figure S3G), as well as mtOCR (Figure S2). That a clinically relevant dose of 100 nM of MitoQ[8,15] was sufficient to repress doxorubicin-induced migration was confirmed using 168FARN cells (Figure S3G).

MitoTEMPO prevents 4T1 breast cancer lung metastasis in combination with doxorubicin

Our study was concluded by addressing the possibility of metastasis induction by low doses of doxorubicin, which was tested using 4T1 cells in immunocompetent syngeneic mice. Figure 6A depicts our treatment strategy that was aimed to be clinically relevant by (1) using an orthotopic model, (2) starting treatments only after the establishment of palpable breast tumors (Day 0), (3) randomly assigning mice to treatment groups, (4) delivering relevant doses of doxorubicin (4 mg/Kg per week for 3 weeks, i.v.)[25] and of MitoTEMPO (0.7 mg/Kg per day for 3 weeks, i.p.), and (5) including single treatment controls as well as a placebo arm. From the day of tumor inoculation (Day −7), 4T1 tumor growth was monitored every 3 days using an electronic caliper. There was no significant difference in primary tumor growth before treatment (Figure 6B). After treatment, either doxorubicin alone or doxorubicin + MitoTEMPO significantly delayed tumor growth ($p < 0.05$), but the combination treatment did not surpass doxorubicin treatment alone. MitoTEMPO alone induced no growth delay.

Fortunately, although doxorubicin increased the expression of phospho-Y402-PYK2 in the tumors (Figure S4), the examination of 4T1-bearing mouse lungs showed no induction of metastasis (Figure 6C, where $p > 0.05$ between control and doxorubicin 4 mg/kg). Yet, doxorubicin did not to prevent metastasis occurrence. Comparatively, MitoTEMPO prevented spontaneous lung metastasis in the presence or not of doxorubicin (Figure 6C). It was associated with a decreased expression of doxorubicin-induced PYK2 phosphorylation on Y402 (Figure S4). Full metastatic prevention was reached upon treatment combination (13/13 mice with background signals), and almost reached with MitoTEMPO alone (4/5 mice). Comparatively, 66.7% (20/30) and 71.9% (23/32) of mice were positive

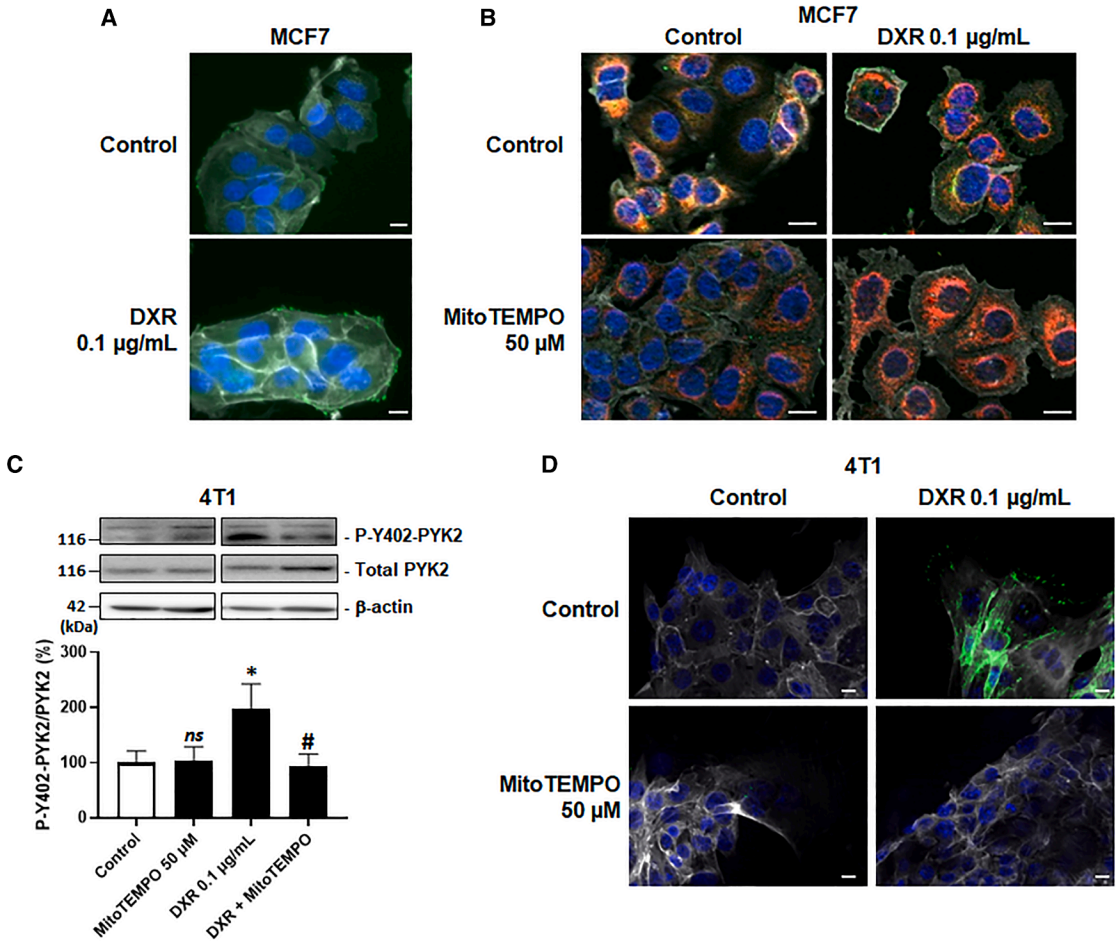

Figure 4. MitoTEMPO inhibits doxorubicin-induced activation of the downstream part of the TGFβ signaling pathway

(A) Representative pictures of MCF7 breast cancer cells that were treated for 24 h with 0.1 μg/mL doxorubicin (DXR), and stained with a specific anti-phospho-Y402-Pyk2 antibody (green). Nuclei were stained with DAPI (blue). Bars = 10 μm.

(B) Representative pictures of MCF7 cells that were treated for 24 h with 0.1 μg/mL DXR ± 50 μM MitoTEMPO, after which cells were stained with a specific anti-phospho-Y402-Pyk2 (green). Mitochondria were stained with MitoTracker Orange (red) and cell nuclei with DAPI (blue). Bars = 20 μm.

(C) 4T1 breast cancer cells were treated with 0.1 μg/mL of DXR for 16 h, left to recover for 6 h, and treated overnight with 50 μM of MitoTEMPO. Representative western blots show phospho-Y402-PYK2 and total PYK2 expression. PYK2 activity is shown as the phospho-Y402-PYK2/total PYK2 ratio in the graph ($n = 6–10$). *ns* $p > 0.05$, $^{*}p < 0.05$, compared to control; $^{\#}p < 0.05$, compared to DXR alone; by one-way ANOVA.

(D) 4T1 cells were treated for 24 h with 0.1 μg/mL DXR ± 50 μM MitoTEMPO, after which cells were stained with a specific anti-phospho-Y402-Pyk2 (green). The cytoskeleton was stained with DyLight 488 phalloidin (white) and cell nuclei with DAPI (blue). Bars = 10 μm.

for metastasis in the control and doxorubicin alone treatment arms, respectively.

DISCUSSION

This study was aimed to test the possibility that exposure of breast cancer cells to subcytotoxic levels of anthracyclines could promote metastasis. Clinically, such an event could occur in poorly perfused tumor areas of patients treated with chemotherapy.[20] According to the hypothesis, we report using two human and one murine breast cancer cell lines that low doses of doxorubicin trigger cancer cell migration and invasion in a mtROS-dependent manner. Hopefully, these prometastatic gains were insufficient to trigger metastasis in immunocompetent mice, thus ruling out metastatic induction as a side effect of anthracycline-based chemotherapy. Yet, doxorubicin administration alone did not prevent metastasis, while this was achieved in combination with MitoTEMPO or MitoQ, two drugs known to interfere with mtROS production.[12,13] Such combination is clinically relevant, as doses of MitoQ that are achievable in patients did totally prevent spontaneous metastasis from orthotopic breast cancer, and MitoQ did not interfere with doxorubicin-induced cancer cell killing. At the bioactive dose range, MitoQ previously proved to be safe in Phase I clinical trials, with mild headache as a most common side effect and no other serious adverse effect,[15] making of this drug, in our opinion, a strong candidate for metastasis prevention in breast cancer.

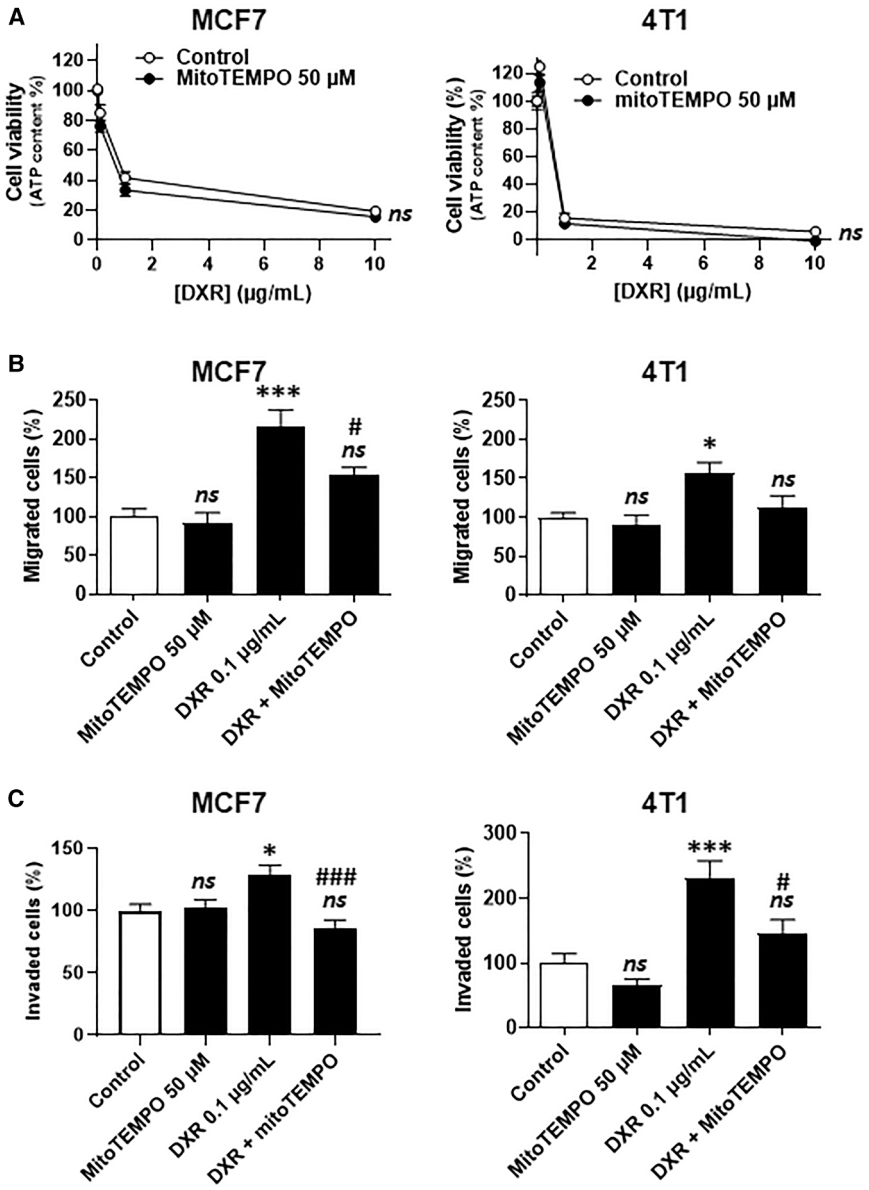

Figure 5. MitoTEMPO inhibits doxorubicin-induced breast cancer cell migration and invasion

(A) MCF7 (left, $n = 24$) and 4T1 (right, $n = 12$) breast cancer cells were treated for 48 h with increasing concentrations of doxorubicin (DXR) ± 50 µM MitoTEMPO, after which cell viability was determined using a luminescent assay that reports on intracellular ATP content. Data are represented as mean ± SEM. *ns* $p > 0.05$, by two-way ANOVA.

(B) Cells were pretreated with ± 0.1 µg/mL DXR ± 50 µM MitoTEMPO for 16 h, and left to recover for 6 h. The graphs show MCF7 (left, $n = 6$) and 4T1 (right, $n = 6$) cell migration toward serum used as a chemoattractant, quantified using a NeuroProbe chemotaxis chamber. Data are represented as mean ± SEM. *ns* $p > 0.05$, $^{*}p < 0.05$, $^{***}p < 0.005$ compared to control; $^{\#}p < 0.05$ compared to DXR treatment alone; by one-way ANOVA with Dunnett's post-hoc test.

(C) As in (B) but testing cell invasion using Matrigel-coated Transwells with Corning Falcon 24-well plates (MCF7, $n = 4$–6; 4T1, $n = 4$–5). Data are represented as mean ± SEM. *ns* $p > 0.05$, $^{*}p < 0.05$, $^{***}p < 0.005$ compared to control; $^{\#}p < 0.05$, $^{\#\#\#}p < 0.005$ compared to DXR treatment alone; by one-way ANOVA with Dunnett's post-hoc test.

See also Figures S2 and S3.

Cancer cells in solid tumors are submitted to a microenvironmental pressure that comprises spatial and temporal fluctuations in oxygen and metabolite bioavailability, fluctuations in the clearance of metabolic wastes, ionic and osmotic alterations, extracellular matrix remodeling, and immune assaults.[32–34] These various elements collectively, progressively and variably produce hostile areas refraining cancer cell proliferation and potentially impairing cell survival. There, cancer cells have at least three different options to survive and reset their aggressive program: shielding through stemness,[35] adapting, and evolving.[36,37] These mechanisms are exacerbated upon therapeutic interventions, accounting for resistance, regrowth, and/or local recurrence, which constitute main causes of clinical treatment failure. A fourth option for cancer cells is escaping, which naturally develops with time in all malignant tumors, accounting for local invasion and distant metastasis.[38] In the present work, we conceived that chemotherapy, already known to promote stemness, adaptation, and evolutive selection,[39–41] could also promote escape. This possibility was tested using breast cancer cells (a type of cancer prone to metastasis) treated with low doses of doxorubicin. Drug selection was based on clinical considerations, with anthracyclines (doxorubicin, epirubicin) together with taxanes being the most active and most frequently used compounds to treat breast cancer. The low concentrations that we tested correspond to those reported in poorly vascularized areas of clinical breast tumors,[23] which may explain the high variability of doxorubicin levels in solid tumors.[20]

Subcytotoxic doses of doxorubicin shifted breast cancer cell metabolism to a more oxidative phenotype (as previously reported by Souid et al.[42] in Jurkat immortalized T human lymphocytes and HL-60 human leukemia cells) associated with an increased electron leak from the mitochondrial ETC and an elevation in mtROS production. This was worrying but not unexpected, as doxorubicin has a high affinity for cardiolipin[21] with, as consequences, a reversible alteration of inner mitochondrial membrane integrity, proton leak, a compensatory increase in cell respiration, increased electron leak, and, ultimately, increased mtROS production exceeding mitochondrial redox defense capacity. MCF7 cancer cells adapted by decreasing

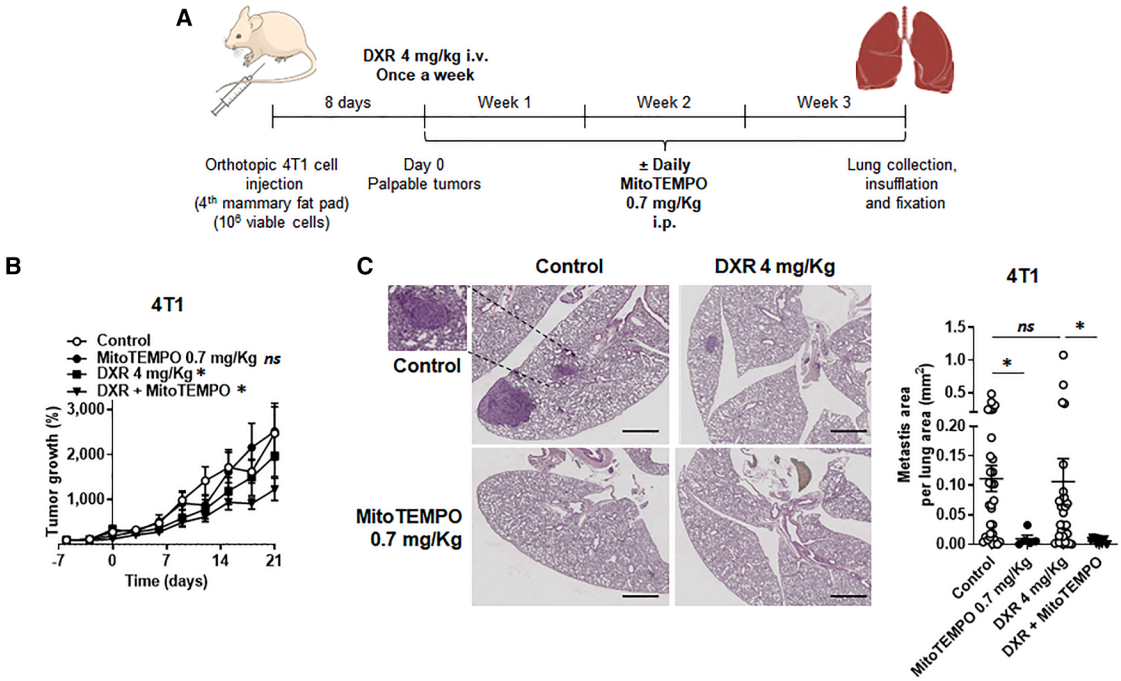

Figure 6. MitoTEMPO prevents 4T1 breast cancer lung metastasis in combination with doxorubicin

(A) Schematic representation of 4T1 breast cancer-bearing immunocompetent syngeneic mice treated with a clinically relevant dose of doxorubicin (DXR) ± MitoTEMPO.

(B and C) Mice were treated following the protocol depicted in (A). (B) The graph shows primary orthotopic breast tumor growth over time (n = 12–16 mice per group). Data are represented as mean ± SEM. *ns* $p > 0.05$, *$p < 0.05$ compared to control, by two-way ANOVA. (C) Mice were euthanized, and metastatic lung colonization was quantified based on the analysis of serial tissue slices on a Leica SCN400 slide scanner. Representative pictures on the left show mouse lungs stained with hematoxylin and eosin (H&E), with the inset focused on a metastatic lesion. Bars = 500 μm. The graph on the right reports on metastasis-positive areas normalized to whole analyzed lung areas (n = 5–32 mice per group). Data are represented as mean ± SEM. *ns* $p > 0.05$, *$p < 0.05$, by Kruskal-Wallis test with Dunn's post-hoc test.

See also Figure S4.

lactate release with unchanged glucose uptake, while 4T1 cells increased glucose uptake with unchanged lactate release. These responses may represent adaptive metabolic strategies to redirect glucose metabolism toward the pentose phosphate and the serine pathways producing antioxidants NADPH and NADH, respectively, capable to inactivate mtROS. Hence, it would be interesting even if materially challenging *in vivo* to measure the redox state of glutathione, thioredoxins, and peroxiredoxins in the mitochondrial fraction of cancer cells exposed to sublethal concentrations of doxorubicin. Differences in the metabolic responses of MCF7 and 4T1 cells may further reflect damage to the TCA cycle affecting the malate-pyruvate-lactate pathway, as MCF7 cells are known to be strongly dependent on oxidative glutaminolysis for survival,[43] while 4T1 cells would be less.

Considering these metabolic changes, our main concern was based on the previous evidence that elevated mtROS levels can induce breast cancer cell migration, invasion, and metastasis.[6–8] We therefore theorized a worst-case scenario for anthracyclines, associating cancer cell killing as an intention with metastasis as a side effect. Our initial results were supportive of this hypothesis, with evidence in three unrelated breast cancer cell lines that low-dose doxorubicin activates focal adhesion kinase PYK2 (the final effector of the TGFβ pathway) induces partial EMT, and triggers migration and invasion. We did not further explore EMT because of the well-established link between elevated mtROS levels and partial EMT in breast cancer cells[44] and the dispensability of EMT for sublethal concentrations of doxorubicin to induce breast cancer cell migration and invasion.[45] A causal link between metabolic changes and the acquisition of a prometastatic phenotype was established by targeting mtROS with MitoTEMPO, resulting in a total loss of migration and invasion gains. It was associated with an inhibition of doxorubicin-induced cancer cell respiration known to reduce mtROS production,[6,7] which can be explained by the capability of MitoTEMPO (and to a larger extent MitoQ) to reduce the electron flux within the ETC by directly intercepting electrons.[46] Of note, MitoTEMPO alone did not block doxorubicin-independent basal migration in our model cell lines, with two possible explanations: (1) the doses of MitoTEMPO that we tested could have been suboptimal to fully block mtROS-dependent migration and/or (2) the basal migration of MCF7 and 4T1 breast cancer cells could be mtROS-independent. Globally, we propose that mitochondria-targeted antioxidants have the potential simultaneously reduce cardiotoxicity[47] and metastasis (this study) in breast cancer patients treated with doxorubicin.

Our *in vivo* observations in immunocompetent mice were reassuring on the one hand and worrying on the other hand. Positive information with respect to clinical applications was that doxorubicin did not promote metastasis *in vivo*. This could be related to the fact that, in addition to migratory and invasive capabilities, metastatic progenitor cells must also possess strong antioxidants and anti-immune defenses to survive in the blood stream and must acquire stem cell characteristics to successfully generate metastases.[38] Doxorubicin could not be potent enough to activate the full metastatic cascade. Further in encouraging findings was that scavenging mtROS with MitoTEMPO did not interfere with the anticancer activity of doxorubicin, indicating that mitochondria-targeted antioxidants can be combined with this type of chemotherapy. In other words, mtROS production was dispensable for delaying tumor growth in our model. Any future clinical transfer will nevertheless depend on confirmation using additional models and other mitochondria-targeted antioxidants, including MitoQ. Worrying was the observation that doxorubicin had no inhibitory effect on metastasis dissemination, which can be linked to the fact that the majority of breast cancer patients reach the metastatic state, even under chemotherapy.[3] Epidemiologic studies are now needed to confirm that anthracyclines do not promote metastasis on the long term. Perhaps the most encouraging information was that MitoTEMPO was extremely efficient to prevent metastasis in our model. Together with independent observations in human breast cancer[6,8] and human pancreatic cancer[11] mouse models, we believe that this observation is a strong incentive for the clinical evaluation of mitochondria-targeted antioxidants for metastasis prevention.

Limitations of the study

In an interesting parallelism with the mitochondrial response of cancer cells, cardiotoxicity by doxorubicin is partially attributed to increased mtROS production by cardiomyocytes, which causes apoptosis.[44] Mechanistically, doxorubicin as a cation accumulates in cardiomyocyte mitochondria where it sequentially irreversibly binds to cardiolipin, disrupts the mitochondrial potential, increases electron leak at ETC Complex I, and thereby increases $mtO_2^{\cdot-}$production.[48] Doxorubicin can also chelate iron, forming complexes that further increase ROS production and cardiotoxicity.[49] However, while cardiotoxicity and cancer cell killing are both linked to induction of mitochondrial dysfunction at clinical doses of doxorubicin, the promigratory and pro-invasive effects of subclinical doses of the drug that we report here were rather associated with a gain in mtOCR. This could be explained by the remarkable capability of cancer cells to increase mitochondrial turnover (fission, mitophagy, mitochondrial biogenesis, and fusion) upon mitochondrial damage, which participates in chemoresistance.[50,51] Whether subcytotoxic doses of doxorubicin trigger mitochondrial turnover in breast cancer cells is currently unknown. We believe that it warrants further investigation, especially in the context of both escape and chemoresistance.

Finally, we observed no prometastatic effects of doxorubicin and antimetastatic effects of MitoTEMPO in immunocompetent mice, in which both drugs could exert immunomodulatory effects in addition to direct effects on cancer cells.[52–54] While we chose immunocompetent models for their clinical relevance, we believe that exploring the contribution of antitumor immunity to the global responses that we observed is of particular interest.

RESOURCE AVAILABILITY

Lead contact

Further information and requests for resources and reagents should be directed to and will be fulfilled by the lead contact, Pierre Sonveaux (pierre.sonveaux@uclouvain.be).

Materials availability

This study did not generate new unique reagents.

Data and code availability

This paper does not report an original code. Any additional information required to reanalyze the data reported in this paper is available from the lead contact upon request.

ACKNOWLEDGMENTS

This work was supported by the FRFS-WELBIO strategic axis of the Walloon Region of Belgium (WELBIO-CR-2022A-13), European Union's FP7/2007-2013 ERC Independent Researcher Starting Grant 243188 TUMETABO, European Union's Horizon 2020 research innovation program under the Marie Skłodowska-Curie grant agreement no. 722605 TRANSMIT, the Actions de Recherche Concertées program of the Communauté Française de Belgique (ARC 09/14-020, 14/19-058), the Fondation Belge contre le Cancer (Fundamental Research grant nos. F86 and FAF-F/2018/1282), the Belgian Fonds National de la Recherche Scientifique (FRS-FNRS; grant nos. FRSM 3.4567.10, FRFC 2.5025.12, and CDR J.0135.18), the Belgian Télévie (grant nos. 7.4508.14 and 7.4529.17), the Louvain Foundation, and the UCLouvain Fonds Spéciaux de la Recherche (FSR) to P.S.; Fondazione AIRC per la Ricerca sul Cancro (AIRC-IG #30515) to P.E.P.; and Ricerca Finalizzata, Ministero della Salute (GR-2021-12374957) to G.C. L.X.Z. is a PhD Fellow of Marie Skłodowska-Curie grant no. 722605 TRANSMIT. V.L.P. is a PhD Fellow and P. S. is a Research Director of the F.R.S.-FNRS. P.S. is a WELBIO Investigator. Authors thank the Cliniques Universitaires Saint-Luc (CUSL) for the kind provision of doxorubicin hydrochloride, Michael P. Murphy (University of Cambridge, UK) for the kind gift of MitoQ, and Fred R. Miller (Karmanos Cancer Institute, Detroit, MI, USA) for providing 4T1 and 168FARN breast cancer cells. Authors also thank Caroline Bouzin (UCLouvain IREC Imaging 2IP Platform) and Davide Brusa (UCLouvain IREC Flow Cytometry and Cell Sorting Platform) for technological assistance and training, and Emmanuel Vandenhooft for animal care.

AUTHOR CONTRIBUTIONS

Conceptualization, P.E.P. and P.S.; methodology, V.L.P., P.E.P., and P.S.; investigation, T.C., J.A.V.d.V., E.P., L.I., L.X.Z., M.T., T.V., A.P., G.C., A.S., V.L.P., and P.E.P.; formal analysis, T.C., J.A.V.d.V., E.P., L.I., L.X.Z., G.C., A. S., V.L.P., P.E.P., and P.S.; validation, P.E.P. and P.S.; resources, P.E.P. and P.S.; data curation, P.E.P. and P.S.; writing – original draft preparation, P.E.P. and P.S.; writing – review and editing, T.C., J.A.V.d.V., E.P., L.I., L.X. Z., M.T., T.V., A.P., G.C., A.S., V.L.P., P.E.P., and P.S.; visualization, T.C., J. A.V.d.V., P.E.P., and P.S.; supervision, P.S.; project administration, P.S.; funding acquisition, G.C., P.E.P., and P.S. All authors have read and agreed the submitted version of the manuscript.

DECLARATION OF INTERESTS

T.C. and P.S. are inventors of patent application WO2022/243541 "Molecular signature for assessing the responsiveness of cancer to mitochondria-targeted antioxidants". P.S. is inventor of patent application EP24186067.5 "Mitochondrially-targeted antioxidant compound for use in radiation therapy". P. S. is involved in a clinical collaboration with Antipodean Pharmaceuticals Inc.

for the prevention of breast cancer metastasis. Authors declare no other conflict of interest. In particular, Antipodean Pharmaceuticals Inc. and MitoQ Inc., who possess patent rights on the MitoQ molecule, did not fund the study. Neither them nor the funders were involved in the design of the study; in the collection, analyses, or interpretation of data; in the writing of the manuscript; or in the decision to publish the results.

STAR★METHODS

Detailed methods are provided in the online version of this paper and include the following:

- KEY RESOURCES TABLE
- EXPERIMENTAL MODEL AND STUDY PARTICIPANT DETAILS
  - Cells and culture conditions
  - Mice and mouse experiments
- METHOD DETAILS
  - Chemicals and reagents
  - Cell numbers and viability
  - Clonogenic assays
  - Microscopy
  - Metabolic assays
  - Cell migration and invasion assays
  - Western blotting
  - Real-time quantitative PCR
  - Statistical analysis

SUPPLEMENTAL INFORMATION

Supplemental information can be found online at https://doi.org/10.1016/j.isci.2025.113031.

Received: January 6, 2025
Revised: May 21, 2025
Accepted: June 26, 2025
Published: June 28, 2025

REFERENCES

1. Steeg, P.S. (2016). Targeting metastasis. Nat. Rev. Cancer *16*, 201–218. https://doi.org/10.1038/nrc.2016.25.
2. Dillekas, H., Rogers, M.S., and Straume, O. (2019). Are 90% of deaths from cancer caused by metastases? Cancer Med. *8*, 5574–5576. https://doi.org/10.1002/cam4.2474.
3. Xiao, W., Zheng, S., Yang, A., Zhang, X., Zou, Y., Tang, H., and Xie, X. (2018). Breast cancer subtypes and the risk of distant metastasis at initial diagnosis: a population-based study. Cancer Manag. Res. *10*, 5329–5338. https://doi.org/10.2147/CMAR.S176763.
4. Steeg, P.S. (2006). Tumor metastasis: mechanistic insights and clinical challenges. Nat. Med. *12*, 895–904. https://doi.org/10.1038/nm1469.
5. Semenza, G.L. (2016). The hypoxic tumor microenvironment: a driving force for breast cancer progression. Biochim. Biophys. Acta *1863*, 382–391. https://doi.org/10.1016/j.bbamcr.2015.05.036.
6. Porporato, P.E., Payen, V.L., Pérez-Escuredo, J., De Saedeleer, C.J., Danhier, P., Copetti, T., Dhup, S., Tardy, M., Vazeille, T., Bouzin, C., et al. (2014). A mitochondrial switch promotes tumor metastasis. Cell Rep. *8*, 754–766. https://doi.org/10.1016/j.celrep.2014.06.043.
7. Capeloa, T., Krzystyniak, J., d'Hose, D., Canas Rodriguez, A., Payen, V.L., Zampieri, L.X., Van de Velde, J.A., Benyahia, Z., Pranzini, E., Vazeille, T., et al. (2022). MitoQ inhibits human breast cancer cell migration, invasion and clonogenicity. Cancers (Basel) *14*, 1516. https://doi.org/10.3390/cancers14061516.
8. Capeloa, T., Krzystyniak, J., Rodriguez, A.C., Payen, V.L., Zampieri, L.X., Pranzini, E., Derouane, F., Vazeille, T., Bouzin, C., Duhoux, F.P., et al. (2022). MitoQ prevents human breast cancer recurrence and lung metastasis in mice. Cancers (Basel) *14*, 1488. https://doi.org/10.3390/cancers14061488.
9. Tokarska-Schlattner, M., Zaugg, M., Zuppinger, C., Wallimann, T., and Schlattner, U. (2006). New insights into doxorubicin-induced cardiotoxicity: the critical role of cellular energetics. J. Mol. Cell. Cardiol. *41*, 389–405. https://doi.org/10.1016/j.yjmcc.2006.06.009.
10. Ishikawa, K., Takenaga, K., Akimoto, M., Koshikawa, N., Yamaguchi, A., Imanishi, H., Nakada, K., Honma, Y., and Hayashi, J.I. (2008). ROS-generating mitochondrial DNA mutations can regulate tumor cell metastasis. Science *320*, 661–664. https://doi.org/10.1126/science.1156906.
11. Capeloa, T., Van de Velde, J.A., d'Hose, D., Lipari, S.G., Derouane, F., Hamelin, L., Bedin, M., Vazeille, T., Duhoux, F.P., Murphy, M.P., et al. (2022). Inhibition of mitochondrial redox signaling with MitoQ prevents metastasis of human pancreatic cancer in mice. Cancers (Basel) *14*, 4918. https://doi.org/10.3390/cancers14194918.
12. Dikalova, A.E., Bikineyeva, A.T., Budzyn, K., Nazarewicz, R.R., McCann, L., Lewis, W., Harrison, D.G., and Dikalov, S.I. (2010). Therapeutic targeting of mitochondrial superoxide in hypertension. Circ. Res. *107*, 106–116. https://doi.org/10.1161/CIRCRESAHA.109.214601.
13. Kelso, G.F., Porteous, C.M., Coulter, C.V., Hughes, G., Porteous, W.K., Ledgerwood, E.C., Smith, R.A., and Murphy, M.P. (2001). Selective targeting of a redox-active ubiquinone to mitochondria within cells: antioxidant and antiapoptotic properties. J. Biol. Chem. *276*, 4588–4596. https://doi.org/10.1074/jbc.M009093200.
14. James, A.M., Cochemé, H.M., Smith, R.A.J., and Murphy, M.P. (2005). Interactions of mitochondria-targeted and untargeted ubiquinones with the mitochondrial respiratory chain and reactive oxygen species. Implications for the use of exogenous ubiquinones as therapies and experimental tools. J. Biol. Chem. *280*, 21295–21312. https://doi.org/10.1074/jbc.M501527200.
15. Smith, R.A.J., and Murphy, M.P. (2010). Animal and human studies with the mitochondria-targeted antioxidant MitoQ. Ann. N. Y. Acad. Sci. *1201*, 96–103. https://doi.org/10.1111/j.1749-6632.2010.05627.x.
16. Payen, V.L., Zampieri, L.X., Porporato, P.E., and Sonveaux, P. (2019). Pro- and antitumor effects of mitochondrial reactive oxygen species. Cancer Metastasis Rev. *38*, 189–203. https://doi.org/10.1007/s10555-019-09789-2.
17. Davies, K.J., and Doroshow, J.H. (1986). Redox cycling of anthracyclines by cardiac mitochondria. I. Anthracycline radical formation by NADH dehydrogenase. J. Biol. Chem. *261*, 3060–3067. https://doi.org/10.1016/S0021-9258(17)35746-0.
18. Doroshow, J.H., and Davies, K.J. (1986). Redox cycling of anthracyclines by cardiac mitochondria. II. Formation of superoxide anion, hydrogen peroxide, and hydroxyl radical. J. Biol. Chem. *261*, 3068–3074. https://doi.org/10.1016/S0021-9258(17)35747-2.
19. Goormaghtigh, E., Huart, P., Praet, M., Brasseur, R., and Ruysschaert, J. M. (1990). Structure of the adriamycin-cardiolipin complex. Role in mitochondrial toxicity. Biophys. Chem. *35*, 247–257. https://doi.org/10.1016/0301-4622(90)80012-v.
20. Rossi, C., Gasparini, G., Canobbio, L., Galligioni, E., Volpe, R., Candiani, E., Toffoli, G., and D'Incalci, M. (1987). Doxorubicin distribution in human breast cancer. Cancer Treat Rep. *71*, 1221–1226.
21. Goormaghtigh, E., Chatelain, P., Caspers, J., and Ruysschaert, J.M. (1980). Evidence of a complex between adriamycin derivatives and cardiolipin: possible role in cardiotoxicity. Biochem. Pharmacol. *29*, 3003–3010. https://doi.org/10.1016/0006-2952(80)90050-7.
22. Abdullah, C.S., Alam, S., Aishwarya, R., Miriyala, S., Bhuiyan, M.A.N., Panchatcharam, M., Pattillo, C.B., Orr, A.W., Sadoshima, J., Hill, J.A., and Bhuiyan, M.S. (2019). Doxorubicin-induced cardiomyopathy associated with inhibition of autophagic degradation process and defects in mitochondrial respiration. Sci. Rep. *9*, 2002. https://doi.org/10.1038/s41598-018-37862-3.

23. Saeki, T., Nomizu, T., Toi, M., Ito, Y., Noguchi, S., Kobayashi, T., Asaga, T., Minami, H., Yamamoto, N., Aogi, K., et al. (2007). Dofequidar fumarate (MS-209) in combination with cyclophosphamide, doxorubicin, and fluorouracil for patients with advanced or recurrent breast cancer. J. Clin. Oncol. *25*, 411–417. https://doi.org/10.1200/JCO.2006.08.1646.

24. Brookes, P.S. (2005). Mitochondrial H(+) leak and ROS generation: an odd couple. Free Radic. Biol. Med. *38*, 12–23. https://doi.org/10.1016/j.freeradbiomed.2004.10.016.

25. Bandyopadhyay, A., Wang, L., Agyin, J., Tang, Y., Lin, S., Yeh, I.T., De, K., and Sun, L.Z. (2010). Doxorubicin in combination with a small TGFbeta inhibitor: a potential novel therapy for metastatic breast cancer in mouse models. PLoS One *5*, e10365. https://doi.org/10.1371/journal.pone.0010365.

26. Li, D., Xia, L., Huang, P., Wang, Z., Guo, Q., Huang, C., Leng, W., and Qin, S. (2023). Heterogeneity and plasticity of epithelial-mesenchymal transition (EMT) in cancer metastasis: Focusing on partial EMT and regulatory mechanisms. Cell Prolif. *56*, e13423. https://doi.org/10.1111/cpr.13423.

27. Kemble, D.J., and Sun, G. (2009). Direct and specific inactivation of protein tyrosine kinases in the Src and FGFR families by reversible cysteine oxidation. Proc. Natl. Acad. Sci. USA *106*, 5070–5075. https://doi.org/10.1073/pnas.0806117106.

28. Ramundo, V., Giribaldi, G., and Aldieri, E. (2021). Transforming growth factor-beta and oxidative stress in cancer: a crosstalk in driving tumor transformation. Cancers (Basel) *13*, 3093. https://doi.org/10.3390/cancers13123093.

29. Wendt, M.K., Schiemann, B.J., Parvani, J.G., Lee, Y.H., Kang, Y., and Schiemann, W.P. (2013). TGF-beta stimulates Pyk2 expression as part of an epithelial-mesenchymal transition program required for metastatic outgrowth of breast cancer. Oncogene *32*, 2005–2015. https://doi.org/10.1038/onc.2012.230.

30. Porporato, P.E., and Sonveaux, P. (2015). Paving the way for therapeutic prevention of tumor metastasis with agents targeting mitochondrial superoxide. Mol. Cell. Oncol. *2*, e968043. https://doi.org/10.4161/23723548.2014.968043.

31. Snow, B.J., Rolfe, F.L., Lockhart, M.M., Frampton, C.M., O'Sullivan, J.D., Fung, V., Smith, R.A.J., Murphy, M.P., and Taylor, K.M.; Protect Study Group (2010). A double-blind, placebo-controlled study to assess the mitochondria-targeted antioxidant MitoQ as a disease-modifying therapy in Parkinson's disease. Mov. Disord. *25*, 1670–1674. https://doi.org/10.1002/mds.23148.

32. Gane, E.J., Weilert, F., Orr, D.W., Keogh, G.F., Gibson, M., Lockhart, M.M., Frampton, C.M., Taylor, K.M., Smith, R.A.J., and Murphy, M.P. (2010). The mitochondria-targeted anti-oxidant mitoquinone decreases liver damage in a phase II study of hepatitis C patients. Liver Int. *30*, 1019–1026. https://doi.org/10.1111/j.1478-3231.2010.02250.x.

33. Justus, C.R., Dong, L., and Yang, L.V. (2013). Acidic tumor microenvironment and pH-sensing G protein-coupled receptors. Front. Physiol. *4*, 354. https://doi.org/10.3389/fphys.2013.00354.

34. Montenegro, F., and Indraccolo, S. (2020). Metabolism in the tumor microenvironment. Adv. Exp. Med. Biol. *1263*, 1–11. https://doi.org/10.1007/978-3-030-44518-8_1.

35. Hass, R., von der Ohe, J., and Ungefroren, H. (2020). Impact of the tumor microenvironment on tumor heterogeneity and consequences for cancer cell plasticity and stemness. Cancers (Basel) *12*, 3716. https://doi.org/10.3390/cancers12123716.

36. Fendt, S.M., Frezza, C., and Erez, A. (2020). Targeting metabolic plasticity and flexibility dynamics for cancer therapy. Cancer Discov. *10*, 1797–1807. https://doi.org/10.1158/2159-8290.CD-20-0844.

37. Persi, E., Wolf, Y.I., Horn, D., Ruppin, E., Demichelis, F., Gatenby, R.A., Gillies, R.J., and Koonin, E.V. (2021). Mutation-selection balance and compensatory mechanisms in tumour evolution. Nat. Rev. Genet. *22*, 251–262. https://doi.org/10.1038/s41576-020-00299-4.

38. Gupta, G.P., and Massagué, J. (2006). Cancer metastasis: building a framework. Cell *127*, 679–695. https://doi.org/10.1016/j.cell.2006.11.001.

39. Ponnusamy, L., Mahalingaiah, P.K.S., Chang, Y.W., and Singh, K.P. (2019). Role of cellular reprogramming and epigenetic dysregulation in acquired chemoresistance in breast cancer. Cancer Drug Resist. *2*, 297–312. https://doi.org/10.20517/cdr.2018.11.

40. Fodale, V., Pierobon, M., Liotta, L., and Petricoin, E. (2011). Mechanism of cell adaptation: when and how do cancer cells develop chemoresistance? Cancer J. *17*, 89–95. https://doi.org/10.1097/PPO.0b013e318212dd3d.

41. Yates, J.W.T., and Mistry, H. (2020). Clone wars: quantitatively understanding cancer drug resistance. JCO Clin. Cancer Inform. *4*, 938–946. https://doi.org/10.1200/CCI.20.00089.

42. Souid, A.K., Penefsky, H.S., Sadowitz, P.D., and Toms, B. (2006). Enhanced cellular respiration in cells exposed to doxorubicin. Mol. Pharm. *3*, 307–321. https://doi.org/10.1021/mp050080j.

43. Timmerman, L.A., Holton, T., Yuneva, M., Louie, R.J., Padró, M., Daemen, A., Hu, M., Chan, D.A., Ethier, S.P., van 't Veer, L.J., et al. (2013). Glutamine sensitivity analysis identifies the xCT antiporter as a common triple-negative breast tumor therapeutic target. Cancer Cell *24*, 450–465. https://doi.org/10.1016/j.ccr.2013.08.020.

44. Monti, E., Mancini, A., Marras, E., and Gariboldi, M.B. (2022). Targeting mitochondrial ROS production to reverse the epithelial-mesenchymal transition in breast cancer cells. Curr. Issues Mol. Biol. *44*, 5277–5293. https://doi.org/10.3390/cimb44110359.

45. Mohammed, S., Shamseddine, A.A., Newcomb, B., Chavez, R.S., Panzner, T.D., Lee, A.H., Canals, D., Okeoma, C.M., Clarke, C.J., and Hannun, Y.A. (2021). Sublethal doxorubicin promotes migration and invasion of breast cancer cells: role of Src Family non-receptor tyrosine kinases. Breast Cancer Res. *23*, 76. https://doi.org/10.1186/s13058-021-01452-5.

46. Rondeau, J.D., Van de Velde, J.A., Bouidida, Y., and Sonveaux, P. (2024). Subclinical dose irradiation triggers human breast cancer migration via mitochondrial reactive oxygen species. Cancer Metab. *12*, 20. https://doi.org/10.1186/s40170-024-00347-1.

47. Sacks, B., Onal, H., Martorana, R., Sehgal, A., Harvey, A., Wastella, C., Ahmad, H., Ross, E., Pjetergjoka, A., Prasad, S., et al. (2021). Mitochondrial targeted antioxidants, mitoquinone and SKQ1, not vitamin C, mitigate doxorubicin-induced damage in H9c2 myoblast: pretreatment vs. co-treatment. BMC Pharmacol. Toxicol. *22*, 49. https://doi.org/10.1186/s40360-021-00518-6.

48. Rawat, P.S., Jaiswal, A., Khurana, A., Bhatti, J.S., and Navik, U. (2021). Doxorubicin-induced cardiotoxicity: An update on the molecular mechanism and novel therapeutic strategies for effective management. Biomed. Pharmacother. *139*, 111708. https://doi.org/10.1016/j.biopha.2021.111708.

49. Jones, I.C., and Dass, C.R. (2022). Doxorubicin-induced cardiotoxicity: causative factors and possible interventions. J. Pharm. Pharmacol. *74*, 1677–1688. https://doi.org/10.1093/jpp/rgac063.

50. Hardy, L., Frison, M., and Campanella, M. (2018). Breast cancer cells exploit mitophagy to exert therapy resistance. Oncotarget *9*, 14040–14041. https://doi.org/10.18632/oncotarget.24533.

51. Jin, P., Jiang, J., Zhou, L., Huang, Z., Nice, E.C., Huang, C., and Fu, L. (2022). Mitochondrial adaptation in cancer drug resistance: prevalence, mechanisms, and management. J. Hematol. Oncol. *15*, 97. https://doi.org/10.1186/s13045-022-01313-4.

52. Huang, F.Y., Lei, J., Sun, Y., Yan, F., Chen, B., Zhang, L., Lu, Z., Cao, R., Lin, Y.Y., Wang, C.C., and Tan, G.H. (2018). Induction of enhanced immunogenic cell death through ultrasound-controlled release of doxorubicin by liposome-microbubble complexes. OncoImmunology *7*, e1446720. https://doi.org/10.1080/2162402X.2018.1446720.

53. Takayama, T., Shimizu, T., Lila, A.S.A., Kanazawa, Y., Ando, H., Ishima, Y., and Ishida, T. (2020). Adjuvant Antitumor Immunity Contributes to the Overall Antitumor effect of pegylated liposomal doxorubicin (Doxil((R))) in C26 tumor-bearing immunocompetent mice. Pharmaceutics *12*, 990. https://doi.org/10.3390/pharmaceutics12100990.

54. Arulkumaran, N., Pollen, S.J., Tidswell, R., Gaupp, C., Peters, V.B.M., Stanzani, G., Snow, T.A.C., Duchen, M.R., and Singer, M. (2021). Selective mitochondrial antioxidant MitoTEMPO reduces renal dysfunction and systemic inflammation in experimental sepsis in rats. Br. J. Anaesth. *127*, 577–586. https://doi.org/10.1016/j.bja.2021.05.036.

55. Mina, E., Wyart, E., Sartori, R., Angelino, E., Zaggia, I., Rausch, V., Maldotti, M., Pagani, A., Hsu, M.Y., Friziero, A., et al. (2023). FK506 bypasses the effect of erythroferrone in cancer cachexia skeletal muscle atrophy. Cell Rep. Med. *4*, 101306. https://doi.org/10.1016/j.xcrm.2023.101306.

56. Zampieri, L.X., Grasso, D., Bouzin, C., Brusa, D., Rossignol, R., and Sonveaux, P. (2020). Mitochondria participate in chemoresistance to cisplatin in human ovarian cancer cells. Mol. Cancer Res. *18*, 1379–1391. https://doi.org/10.1158/1541-7786.MCR-19-1145.

57. Zhou, R., Yazdi, A.S., Menu, P., and Tschopp, J. (2011). A role for mitochondria in NLRP3 inflammasome activation. Nature *469*, 221–225. https://doi.org/10.1038/nature09663.

58. Blackman, M.C.N.M., Capeloa, T., Rondeau, J.D., Zampieri, L.X., Benyahia, Z., Van de Velde, J.A., Fransolet, M., Daskalopoulos, E.P., Michiels, C., Beauloye, C., and Sonveaux, P. (2022). Mitochondrial protein Cox7b is a metabolic sensor driving brain-specific metastasis of human breast cancer cells. Cancers (Basel) *14*, 4371. https://doi.org/10.3390/cancers14184371.

STAR★METHODS

KEY RESOURCES TABLE

REAGENT or RESOURCE	SOURCE	IDENTIFIER
Antibodies		
HRP-conjugated goat anti-rabbit	Jackson ImmunoResearch	111-035-003; RRID: AB_2313567.
HRP-conjugated rabbit anti-goat	Jackson ImmunoResearch	305-035-003; RRID: AB_2339400
HRP-conjugated rabbit anti-mouse	Jackson ImmunoResearch	115-035-003; AB_10015289
PYK2 PYK2, tyrosine 402 phosphorylated	Santa-Cruz Biotechnology Santa-Cruz Biotechnology	sc-1515; RRID: AB_632286 sc-101790
β-actin	Sigma-Aldrich	A5441; RRID: AB_476744
GAPDH	Cell Signaling	2118s; RRID: AB_561053
Chemicals, peptides, and recombinant proteins		
Accutase	ThermoFisher	A1110501
Crystal violet solution	Merck Life Science	V5265
D-glucose	Sigma Aldrich	G7021
DAPI	Merck Life Science	D9542
Dimethyl sulfoxide (DMSO), anhydrous	Merck Life Science	5895690100
Doxorubicin hydrochloride	Pharmacy of the Cliniques Universitaires Saint-Luc (CUSL)	N/A
DyLight 488 phalloidin	ThermoFisher	21833PR
MitoQ	Kind gift from Prof. M.P. Murphy	N/A
MitoSOX	ThermoFischer	M36008
MitoTEMPO	Santa-Cruz Biotechnology	sc-221945
MitoTracker Orange	ThermoFisher	M-7510
Vitronectin	Sigma Aldrich	SRP3186
ROX SYBR Master Mix dTTP Blue	Eurogentec	UF-RSMT-B0701
Critical commercial assays		
CellTiter-Glo luminescent cell viability assay	Promega	G7570
XF Cell Mito Stress kit	Agilent Technologies	103015–100
Glucose enzymatic assays on CMA600	Aurora Borealis	P000023
Lactate enzymatic assays on CMA600	Aurora Borealis	P000024
Experimental models: cell lines		
MCF7	ATCC	HTB-22
4T1	Kind gift of Prof. F.R. Miller	N/A
168FARN	kind gift of Prof. F.R. Miller	N/A
Experimental models: organisms/strains		
Balb/cJRj immunocompetent mice, female	Janvier or Enotivco	N/A
Oligonucleotides		
See Methods: real-time quantitative PCR for oligonucleotide information	ThermoFisher	N/A
NucleoSpin RNA mini kit for RNA purification	Macherey-Nagel	740955.50
High-Capacity cDNA reverse transcription kit	ThermoFisher	4368814
Software and algorithms		
Digital Image Hub	Leica	https://www.life-sciences-europe.com/product/digital-image-hub-enterprise-leica-microsystems-danaher-group-2001-21344.html

(*Continued on next page*)

Continued

REAGENT or RESOURCE	SOURCE	IDENTIFIER
Prism version 10.4.1	Graphpad	https://www.graphpad.com/updates
SoftMax Pro	Molecular Devices	https://www.moleculardevices.com/products/microplate-readers/acquisition-and-analysis-software/softmax-pro-software
ImageJ 1.53q	NIH	https://imagej.net/software/imagej/
Bio-Rad CFX Maestro version 2.3	Biorad	https://www.bio-rad.com/en-be/product/cfx-maestro-software-for-cfx-real-time-pcr-instruments?ID=OKZP7E15
Others		
Agarose	Carl Roth	3810,4
DMEM (Glutamax +4.5 g/L glucose)	Gibco	11965092
Fetal bovine serum (FBS)	Merck Life Science	R-6404352
Matrigel, growth factor-reduced	Merck Life Science	CLS354263

EXPERIMENTAL MODEL AND STUDY PARTICIPANT DETAILS

Cells and culture conditions

Human MCF7 breast cancer cells (ATCC, Manassas, VA, USA; catalog #HTB-22) and murine 4T1 and 168FARN breast cancer cells (kind gifts of Prof. Fred R. Miller, Karmanos Cancer Institute, Detroit, MI, USA) were routinely cultured in DMEM containing Glutamax and 4.5 g/L glucose (Gibco, catalog #11965092), supplemented with 10% FBS in a humidified atmosphere with 5% CO_2, 37°C. Unless stated otherwise, all *in vitro* assays were performed in this medium.

Mice and mouse experiments

Mouse experiments were performed with the approval of UCLouvain Comité d'Ethique pour l'Expérimentation Animale (approval IDs: UCL/MD/2010/11, 2016/UCL/MD/018 and 2020/UCL/MD/033), and the Italian Ministry of Health according to national and European (directive 2010/63/EU) animal care regulations. On Day-8, 9-week-old female balb/cJRj mice (Janvier, Le Genest-Saint-Isle, France, or Enotivco, Italy) were injected with 200,000 viable 4T1 cells into the fourth mammary fat pad. When tumors became palpable in all mice and reached an average diameter of 4 mm (Day 0), doxorubicin (4 mg/kg) was administered intravenously once per week for 3 weeks ± daily intraperitoneal injections of MitoTEMPO (0.7 mg/kg) or vehicle (DMSO) until the end of the experiment. For Figure 6, tumor volumes were determined three times per week using an electronic caliper and normalized to tumor volume at Day 0. At endpoint (Day +21), mice were euthanized by cervical dislocation and their lungs were fixed in formalin. Tissues were stained with hematoxylin & eosin (H&E), pictures of whole lung slides were acquired with a slide scanner (SCN400; Leica Biosystems, Diegem, Belgium), and analyzed with the Digital Image Hub software (Leica Biosystems). The area colonized by metastases was normalized to the total sliced lung area. For Figure S4, mice were euthanized on Day +2 after three daily injections of MitoTEMPO, and the primary tumors were processed for western blotting as previously shown.[55]

METHOD DETAILS

Chemicals and reagents

Doxorubicin hydrochloride was kindly provided by the Pharmacy of the Cliniques Universitaires Saint-Luc (CUSL), Brussels, Belgium. (2-(2,2,6,6-Tetramethylpiperidin-1-oxyl-4-ylamino)-2-oxoethyl)triphenylphosphonium chloride (MitoTEMPO; Santa-Cruz Biotechnology, catalog #sc-221945) was dissolved in anhydrous DMSO to produce a 50 mM stock solution that was stored at −20°C for maximum 30 days. Mitoquinone mesylate (MitoQ; kind gift from Prof. Michael P. Murphy, University of Cambridge, Cambridge, UK) was dissolved in DMSO at a stock concentration of 1 mM. Equal volumes of solvent (DMSO) were used in control experiments.

Cell numbers and viability

Cell numbers were quantified by automatic cell counting on a SpectraMax i3x spectrophotometer equipped with a MiniMax imaging cytometer (Molecular Devices, Munich, Germany), using the SoftMax Pro software (Molecular Devices). Data were normalized to initial plating density. Cells viability was tested in 96-well plates where cells were left to adhere for 16 h. Following adhesion, cells were treated with the indicated compounds for 48 h, after which staining was done with a CellTiter-Glo luminescent cell viability assay (Promega, Leiden, The Netherlands; catalog #G7570) on a Glomax 96 microplate luminometer (Promega), according to supplier's instructions. This method is based on the quantification of intracellular ATP levels.

Clonogenic assays

Soft agar colony formation assays were performed as previously described[7] 16 h after cell treatment with increasing doses of doxorubicin. After 2 weeks, colonies were counted using an Axiovert 40 CFL microscope (Zeiss, Zaventem, Belgium) equipped with an MRC camera (Zeiss). Results are expressed as surviving fraction (SF), where SF = #colonies/plating efficiency.

Microscopy

Bright field images were captured on an Axiovert 25 microscope (Zeiss) on cells that were treated for 16 h ± 0.1 μg/mL doxorubicin in Petri dishes and left to recover for 6 h in full culture medium. For immunocytochemistry, cells plated on glass coverslips were treated with the indicated amounts of drugs for 16 h and left to recover for 6 h in full culture medium. Immunofluorescent staining was then performed on fixed cells as previously described.[56] After cell fixation, permeabilization, blocking, and the use of primary and secondary antibodies, DyLight 488 phalloidin (ThermoFisher, Erembodegem, Belgium; catalog #21833PR), MitoTracker Orange 100 nM (ThermoFisher; catalog #M-7510) and/or 4′,6-diamidino-2-phenylindole dihydrochloride (DAPI; 1 μg/mL) were added directly onto each glass coverslip in a humidified chamber for 30 min. Primary antibodies were a rabbit polyclonal anti-phospho-Tyr402-PYK2 (Santa-Cruz Biotechnology, Heidelberg, Germany; catalog #sc-101790). Secondary antibodies were an Alexa Fluor 488-conjugated goat anti-rabbit (ThermoFisher; catalog #A-11034). Images were captured by structured illumination fluorescence microscopy using an ApoTome-equipped AxioImager.z1 microscope (Zeiss).

Metabolic assays

Cells (40,000) were plated and left to adhere for 24 h before treatment with the indicated doses of doxorubicin. Oxygen consumption rates (OCRs) were determined on a Seahorse XF96 bioenergetic analyzer (Agilent Technologies, Machelen, Belgium) using the XF Cell Mito Stress kit (Agilent Technologies), as previously shown.[11] Glucose and lactate concentrations were measured in cell supernatants using specific enzymatic assays on a CMA600 analyzer (Aurora Borealis, Schoonebeek, The Netherlands), as previously shown.[11] Mitochondrial superoxide levels were measured in cells loaded with 3 μM MitoSOX[57] (ThermoFischer; catalog #M36008) for 10 min at 37°C. Cells were gently detached with accutase (ThermoFisher; catalog #A1110501), resuspended in PBS containing 10 mM *D*-glucose and 2% FBS, and immediately analyzed by flow cytometry using a FACSCanto II flow cytometer (BD Biosciences, Erembodegem, Belgium).

Cell migration and invasion assays

Cells were pretreated with the indicated amounts of drugs for 16 h and left to recover for 6 h in full culture medium. Migration assays were performed in a NeuroProbe standard 48-well chemotaxis chamber (Gaithersburg, MD, USA), which is a type of transwell assay, according to manufacturer's instructions. Briefly, 50,000 cells were seeded in FBS-deprived medium ± MitoTEMPO or ± MitoQ in the upper chamber, and allowed to migrate overnight through an 8-μm pore-size polycarbonate membrane toward medium containing 0.5% FBS for MCF7 and 4T1 cells, or 0.2% FBS for 186FARN cells. Invasion assays were performed overnight using Matrigel-coated Corning Falcon 24-well plates (Avantor, Leuven, Belgium; catalog #62406-198) toward 30% serum for MCF7 cells and 10% serum for 4T1 and 168FARN cells. For MCF7 cells, membranes were previously incubated for 30 min with a solution of 10 μg/mL vitronectin. Migrated/invaded cells were fixed in 4% PFA for 10 min and stained with 100 μL of a 0.23% v/v crystal violet solution for 10 min before counting on a SpectraMax i3x spectrophotometer equipped with a MiniMax imaging cytometer, using the SoftMax Pro software. All data were normalized to vehicle-treated cells (control).

Western blotting

Cells were treated ± doxorubicin for 16 h, left to recover for 6 h in full culture medium, and treated overnight ± MitoTEMPO. Western blotting was then performed as previously described.[11] Primary antibodies were a goat polyclonal anti-PYK2 (Santa-Cruz Biotechnology; catalog #sc-1515) and a rabbit polyclonal anti-phospho-Tyr402-PYK2 (Santa-Cruz Biotechnology; catalog #sc-101790). Secondary antibodies were horseradish peroxidase (HRP)-conjugated AffiniPure goat anti-rabbit (Jackson ImmunoResearch, Uden, The Netherlands; catalog #111-035-003) and rabbit anti-goat (Jackson ImmunoResearch; catalog #305-035-003) IgGs. Full length membrane images are displayed in Figure S5.

Real-time quantitative PCR

Cells were at 50% confluence were treated ± doxorubicin for 16 h, then left to recover for 6 h in their regular culture medium. Total RNA was extracted and processed as previously described.[58] For human MCF7 cells, primers were: for *vimentin* forward 5′-CGG GAG AAA TTG CAG GAG GA-3′, reverse 5′-AAG GTC AAG ACG TGC CAG AG-3'; for *ZEB1* forward 5′-GCC CAA ACT GCA AGA AAC GC-3′, reverse 5′-GTC GCC CAT TCA CAG GTA TCA-3'; for *slug* forward 5′-GAA CTG GAC ACA CAT ACA GTG AT-3′, reverse 5′-ACA GTG ATG GGG CTG TAT GC-3'; for *E-cadherin* forward 5′-CTT TGA CGC CGA GAG CTA CA-3′, reverse 5′-AAA TTC ACT CTG CCC AGG ACG-3'; and for *HPRT* (used for normalization) forward 5′-TGG CGT CGT GAT TAG TGA TG-3′, reverse 5′-CAC CCT TTC CAA ATC CTC AG-3'. For mouse 4T1 cells, primers were: for *N-cadherin* forward 5′-TCC CTG AGA GAT ACA GCG TCA C-3′, reverse 5′-TGC ATG TGC TCT CAA GTG AA-3'; for *E-cadherin* forward 5′-CAA AGT GAC GCT GAA GTC CA-3′, reverse 5′-TAC ACG CTG GGA AAC ATG AG-3'; and for *GAPDH* (used for normalization) forward 5′-TGC ACC ACC ACC TGC TTA GC-3′, reverse 5′-GGA TGC AGG GAT GAT GTT CT-3'. All primers were ordered from ThermoFisher.

Statistical analysis

Results are expressed as mean ± standard error of the mean (SEM) or as a scatterplot showing the means of *n* independent observations. Error bars are sometimes smaller than symbols. Outliers were identified using Dixon's Q test. Data were analyzed using Graphpad Prism version 10.4.1 (San Diego, CA, USA). Student's t test, one-way ANOVA with Dunnett's post-hoc test, two-way ANOVA with Sidak's post-hoc test and Kruskal-Wallis with Dunn's post-hoc test were used where indicated. $p < 0.05$ was considered to be statistically significant.